

Output tracking for a non-minimum phase robotic manipulator^{*}

Thomas Berger^{*} Lukas Lanza^{*}

^{*} *Institut für Mathematik, Universität Paderborn, Warburger Str. 100,
33098 Paderborn, Germany
(e-mail: {thomas.berger, lanza}@math.upb.de).*

Abstract: We exploit a recently developed funnel control methodology for linear non-minimum phase systems to design an output error feedback controller for a nonlinear robotic manipulator, which is not minimum phase. We illustrate the novel control design by a numerical case study, where we simulate end-effector output tracking of the robotic manipulator.

Keywords: nonlinear systems, adaptive control, non-minimum phase, funnel control, underactuated systems

1. INTRODUCTION

Throughout the last two decades funnel control (introduced in Ilchmann et al. (2002)) turned out to be a powerful tool for the treatment of tracking problems in various applications, such as speed control of wind turbine systems Hackl (2014, 2015), termination of fibrillation processes Berger et al. (2021a), control of peak inspiratory pressure Pomprapa et al. (2015), temperature control of chemical reactor models Ilchmann and Trenn (2004), current and voltage control of electrical circuits Berger and Reis (2014), adaptive cruise control Berger and Rauert (2018, 2020) and control of industrial servo-systems Hackl (2017) and underactuated multibody systems Berger et al. (2019). First results for robotic manipulators have been derived in Hackl et al. (2008); Hackl and Kennel (2012). Many of the aforementioned applications are such that their dynamics are minimum phase. Concerning this property, there are some nuances in the literature, see e.g. Ilchmann and Wirth (2013); we call a system minimum phase, if its internal dynamics (in the linear case the zero dynamics) are bounded-input, bounded-output stable.

The objective of funnel control is to design a feedback control law such that in the closed-loop system the tracking error $e(t) = y(t) - y_{\text{ref}}(t)$ evolves within the boundaries of a prescribed performance funnel

$$\mathcal{F}_\varphi := \{ (t, e) \in \mathbb{R}_{\geq 0} \times \mathbb{R}^m \mid \varphi(t) \|e\| < 1 \},$$

which is determined by a so called funnel function φ belonging to a large set of functions

$$\Phi_r := \left\{ \varphi \in C^r(\mathbb{R}_{\geq 0} \rightarrow \mathbb{R}) \left| \begin{array}{l} \varphi, \dot{\varphi}, \dots, \varphi^{(r)} \text{ are bounded,} \\ \varphi(\tau) > 0 \text{ for all } \tau > 0, \\ \text{and } \liminf_{\tau \rightarrow \infty} \varphi(\tau) > 0 \end{array} \right. \right\},$$

where $r \in \mathbb{N}$ is the relative degree of the system. The latter is, roughly speaking the minimal number one has to differentiate the output of a system to obtain the input explicitly; a definition is provided in the subsequent subsection. The boundary of \mathcal{F}_φ is given by $1/\varphi$, a typical

situation is depicted in Fig. 1. Note that, since φ is bounded, the performance funnel is bounded away from zero, which means that there exists $\lambda > 0$ so that $1/\varphi(t) \geq \lambda$ for all $t > 0$. The requirement of bounded φ can also be waived, see the recent work Berger et al. (2021b).

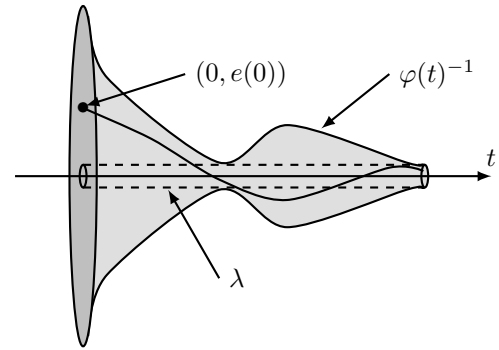


Fig. 1. Error evolution in a funnel \mathcal{F}_φ with boundary $\varphi(t)^{-1}$ for $t > 0$.

Our long-term aim is to study output tracking for nonlinear non-minimum phase systems with known relative degree via funnel control. To achieve this, we seek to exploit a recent result for linear non-minimum phase systems in Berger (2020), where output tracking with prescribed performance is achieved by introducing an auxiliary output. The latter is interpreted as output of a new system with higher relative degree. Using a funnel controller for nonlinear systems with known relative degree as in Berger et al. (2018) and an appropriate new reference signal, tracking with prescribed performance is achieved.

In the present work, we use the ideas and method developed in Berger (2020) to design a controller with which we perform a numerical case study and determine whether the ideas from Berger (2020) are, in principle, feasible for nonlinear systems. We focus on the presentation of a controller design and its numerical validation; feasibility proofs are a topic of future research. As a specific example, we consider end-effector output tracking of a robotic manipulator arm. This example is taken from Seifried and Blajer (2013).

^{*} This work was supported by the German Research Foundation (Deutsche Forschungsgemeinschaft) via the grant BE 6263/1-1.

We emphasize that the robotic manipulator is nonlinear and underactuated, i.e., the system has fewer inputs than degrees of freedom. Further, the internal dynamics are not stable, but have a hyperbolic equilibrium. Moreover, if we treat the internal dynamics as a control system, then a flat output does not exist (cf. Fliess et al. (1995) for flatness). Therefore, the approach from Berger (2020) is not directly feasible. To resolve this, the controller design is based on the linearization of the internal dynamics. Unlike Seifried and Blajer (2013) we use a feedback control law.

A popular open-loop alternative to the approach presented in the present paper is stable system inversion, see Chen and Paden (1996); Devasia et al. (1996). Based on the given reference trajectory, in this method an open-loop (feedforward) control input is calculated. However, for non-minimum phase systems this requires a reverse-time integration, and hence the computed open-loop control input is non-causal. A different approach is based on so called ideal internal dynamics, see Gopalswamy and Hedrick (1993); Shkolnikov and Shtessel (2002). However, this method requires a trackability assumption and sufficient conditions for its feasibility are not available. Stabilization of non-minimum phase systems by dynamic compensators was considered in Isidori (2000) and extended to regulator problems in Marconi et al. (2004); Nazrulla and Khalil (2009), where in the latter work extended high-gain observers are used.

Notation: \mathbb{N} and \mathbb{R} denote the natural and real numbers, resp., $\mathbb{N}_0 = \mathbb{N} \cup \{0\}$ and $\mathbb{R}_{\geq 0} = [0, \infty)$. $C^k(\mathbb{R}_{\geq 0}, \mathbb{R})$ is the (linear) space of k -times continuously differentiable functions $f : \mathbb{R}_{\geq 0} \rightarrow \mathbb{R}$, and $L^\infty(\mathbb{R}_{\geq 0}, \mathbb{R})$ denotes the (linear) space of Lebesgue-measurable and essentially bounded functions. Moreover, $W^{k, \infty}(\mathbb{R}_{\geq 0}, \mathbb{R})$ is the Sobolev space of all functions $f : \mathbb{R}_{\geq 0} \rightarrow \mathbb{R}$ with $f, \dot{f}, \dots, f^{(k)} \in L^\infty(\mathbb{R}_{\geq 0}, \mathbb{R})$, where $k \in \mathbb{N}$. By $\mathbf{GL}_n(\mathbb{R})$ we denote the general linear group of all invertible matrices $A \in \mathbb{R}^{n \times n}$.

2. SYSTEM CLASS AND BYRNES-ISIDORI FORM

We consider nonlinear systems of the form

$$\begin{aligned} \dot{x}(t) &= f(x(t)) + g(x(t))u_d(t), & x(0) &= x^0 \in \mathbb{R}^n, \\ y(t) &= h(x(t)), \end{aligned} \quad (1)$$

with $f : \mathbb{R}^n \rightarrow \mathbb{R}^n$, $g : \mathbb{R}^n \rightarrow \mathbb{R}^{n \times m}$ sufficiently smooth vector fields and $h : \mathbb{R}^n \rightarrow \mathbb{R}^m$ a sufficiently smooth mapping. Further, we assume that $u_d(t) = u(t) + d(t)$, where $u : \mathbb{R}_{\geq 0} \rightarrow \mathbb{R}^m$ and $y : \mathbb{R}_{\geq 0} \rightarrow \mathbb{R}^m$ denote the input and output, resp., and $d : \mathbb{R}_{\geq 0} \rightarrow \mathbb{R}^m$ are bounded disturbances or uncertainties. Disturbances of this kind are expected in real applications, in particular in multibody systems. Note that the dimensions of input and output coincide.

We assume, that system (1) has relative degree $r \in \mathbb{N}$ in the following sense. First, recall the definition of the *Lie derivative* of a function h along a vector field f at a point $z \in U \subseteq \mathbb{R}^n$, U open:

$$(L_f h)(z) := h'(z)f(z),$$

where h' is the Jacobian of h . We may gradually define $L_f^k h = L_f(L_f^{k-1} h)$ with $L_f^0 h = h$. Furthermore, denoting with $g_i(z)$ the columns of $g(z)$ for $i = 1, \dots, m$, we define

$$(L_g h)(z) := [(L_{g_1} h)(z), \dots, (L_{g_m} h)(z)].$$

Now, in virtue of Isidori (1995), the system (1) is said to have relative degree $r \in \mathbb{N}$ on U , if for all $z \in U$ we have:

$$\forall k \in \{0, \dots, r-2\} : (L_g L_f^k h)(z) = 0_{m \times m}$$

$$\text{and } \Gamma(z) := (L_g L_f^{r-1} h)(z) \in \mathbf{GL}_m(\mathbb{R}),$$

where $\Gamma : U \rightarrow \mathbf{GL}_m(\mathbb{R})$ denotes the high-frequency gain matrix.

As mentioned above, in the present paper the design of the controller is based on the linearization of the internal dynamics. Therefore, we have to decouple the internal dynamics first. To this end, we transform system (1) nonlinearly into Byrnes-Isidori form, for details see e.g. Isidori (1995). If system (1) has relative degree $r \in \mathbb{N}$ on an open set $U \subseteq \mathbb{R}^n$, then there exists a (local) diffeomorphism $\Phi : U \rightarrow W \subseteq \mathbb{R}^n$, W open, such that the coordinate transformation $\begin{pmatrix} \xi(t) \\ \eta(t) \end{pmatrix} = \Phi(x(t))$, $\xi(t) \in \mathbb{R}^{rm}$, $\eta(t) \in \mathbb{R}^{n-rm}$ puts system (1) into Byrnes-Isidori form

$$\begin{aligned} y(t) &= \xi_1(t), \\ \dot{\xi}_1(t) &= \xi_2(t), \\ &\vdots \\ \dot{\xi}_{r-1}(t) &= \xi_r(t), \\ \dot{\xi}_r(t) &= (L_f^r h)(\Phi^{-1}(\xi(t), \eta(t))) + \Gamma(\Phi^{-1}(\xi(t), \eta(t)))u_d(t), \\ \dot{\eta}(t) &= q(\xi(t), \eta(t)) + p(\xi(t), \eta(t))u_d(t). \end{aligned} \quad (2)$$

The last equation in (2) represents the internal dynamics of system (1). The diffeomorphism Φ can be represented as

$$\Phi(x) = \begin{pmatrix} h(x) \\ (L_f h)(x) \\ \vdots \\ (L_f^{r-1} h)(x) \\ \phi_1(x) \\ \vdots \\ \phi_{n-rm}(x) \end{pmatrix}, \quad (3)$$

where $\phi_i : U \rightarrow \mathbb{R}$, $i = 1, \dots, n-rm$ are such that $\Phi'(z) \in \mathbf{GL}_n(\mathbb{R})$ for all $z \in U$. If the distribution $\text{im}(g(x))$ in (1) is involutive, then the functions ϕ_i in (3) can additionally be chosen such that

$$\forall i = 1, \dots, n-rm \quad \forall z \in U : (L_g \phi_i)(z) = 0, \quad (4)$$

by which $p(\cdot) = 0$ in (2), cf. (Isidori, 1995, Prop. 5.1.2). Recall from (Isidori, 1995, Sec. 1.3) that $\text{im}(g(x))$ is involutive, if for all smooth vector fields $g_1, g_2 : \mathbb{R}^n \rightarrow \mathbb{R}^n$ with $g_i(x) \in \text{im}(g(x))$ for all $x \in \mathbb{R}^n$ and $i = 1, 2$ we have that the Lie bracket $[g_1, g_2](x) = g_1'(x)g_2(x) - g_2'(x)g_1(x)$ satisfies $[g_1, g_2](x) \in \text{im}(g(x))$ for all $x \in \mathbb{R}^n$.

3. ROTATIONAL MANIPULATOR ARM

To illustrate our approach, in the present paper we consider an underactuated rotational manipulator arm as in Seifried and Blajer (2013), depicted in Fig. 2. The manipulator arm consists of two equal links with homogeneous mass distribution, mass m , length l and inertia $I = l^2 m / 12$. The two links are coupled via a passive joint consisting of a linear spring-damper combination with spring constant c , and damping coefficient d . Using a body fixed coordinate system the tracking point S on the passive link is described by $0 \leq s \leq l$. The control input is chosen as a torque $u = T$ acting on the first link.

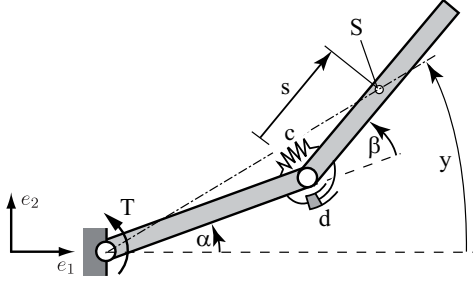


Fig. 2. Rotational manipulator arm with two links and a passive joint. The figure is taken from Seifried and Blajer (2013).

Define $\mathfrak{B} := \{ \beta \in [-\pi, \pi) \mid \cos(\beta) > 2/3 \}$ and $U_\beta := \mathbb{R} \times \mathfrak{B} \times \mathbb{R}^2$. Then, as we will see soon, it is reasonable to consider the dynamics of the manipulator on the set U_β , i.e., the angle $\beta(t)$ is restricted to \mathfrak{B} . Next, we present the equations of motion of the manipulator arm. With

$$\begin{aligned} M : U_\beta &\rightarrow \mathbb{R}^{2 \times 2}, \\ (x_1, \dots, x_4) &\mapsto l^2 m \begin{bmatrix} \frac{5}{3} + \cos(x_2) & \frac{1}{3} + \frac{1}{2} \cos(x_2) \\ \frac{1}{3} + \frac{1}{2} \cos(x_2) & \frac{1}{3} \end{bmatrix}, \\ f_1 : U_\beta &\rightarrow \mathbb{R}, \\ (x_1, \dots, x_4) &\mapsto \frac{1}{2} l^2 m x_4 (2x_3 + x_4) \sin(x_2), \\ f_2 : U_\beta &\rightarrow \mathbb{R}, \\ (x_1, \dots, x_4) &\mapsto -c x_2 - d x_4 - \frac{1}{2} l^2 m x_3^2 \sin(x_2) \end{aligned}$$

the equations of motion are given by

$$\begin{aligned} M(\alpha(t), \beta(t), \dot{\alpha}(t), \dot{\beta}(t)) \begin{pmatrix} \ddot{\alpha}(t) \\ \ddot{\beta}(t) \end{pmatrix} \\ = \begin{pmatrix} f_1(\alpha(t), \beta(t), \dot{\alpha}(t), \dot{\beta}(t)) \\ f_2(\alpha(t), \beta(t), \dot{\alpha}(t), \dot{\beta}(t)) \end{pmatrix} + \begin{bmatrix} 1 \\ 0 \end{bmatrix} u_d(t). \end{aligned} \quad (5)$$

For later use, we compute the inverse of the mass matrix:

$$M(x)^{-1} = \frac{36}{(l^2 m)^2 (16 - 9 \cos^2(x_2))} \begin{bmatrix} \frac{1}{3} & -\frac{1}{3} - \frac{1}{2} \cos(x_2) \\ -\frac{1}{3} - \frac{1}{2} \cos(x_2) & \frac{5}{3} + \cos(x_2) \end{bmatrix}$$

for $x = (x_1, \dots, x_4)^\top \in U_\beta$. As an output for (5) we consider the auxiliary angle

$$y(t) = \alpha(t) + \frac{s}{s+l} \beta(t), \quad (6)$$

which approximates the position S on the passive link for a small angle β . Now, in Seifried and Blajer (2013) it is shown that for this particular output and $s/l > 2/3$ the linearized internal dynamics are unstable. Hence output tracking with $s = l$, i.e., end-effector tracking, leads to unstable internal dynamics, which is the case we are interested in.

To find the relative degree of (5) we calculate the corresponding Lie derivatives. However, this is not directly feasible, since we require a first-order formulation as in (1). We may rewrite (5) in this form with

$$\begin{aligned} f : U_\beta &\rightarrow \mathbb{R}^4, \\ x = (x_1, \dots, x_4) &\mapsto \text{diag}(I_2, M(x)^{-1}) \begin{pmatrix} x_3 \\ x_4 \\ f_1(x) \\ f_2(x) \end{pmatrix}, \\ g : U_\beta &\rightarrow \mathbb{R}^{4 \times 1}, \\ x = (x_1, \dots, x_4) &\mapsto \text{diag}(I_2, M(x)^{-1}) \begin{bmatrix} 0 \\ 0 \\ 1 \\ 0 \end{bmatrix}, \\ h : U_\beta &\rightarrow \mathbb{R}, \\ x = (x_1, \dots, x_4) &\mapsto \left[1, \frac{s}{s+l}, 0, 0 \right] x. \end{aligned}$$

Then, for any $z \in U_\beta$, we obtain the Lie derivatives

$$\begin{aligned} (L_g h)(z) &= \left[1, \frac{s}{s+l}, 0, 0 \right] \text{diag}(I_2, M(z)^{-1}) \begin{bmatrix} 0 \\ 0 \\ 1 \\ 0 \end{bmatrix} = 0, \\ (L_g L_f h)(z) &= (L_f h)'(z) g(z) = (h' f)'(z) g(z) \\ &= \left(\left[1, \frac{s}{s+l}, 0, 0 \right] \text{diag}(I_2, M(z)^{-1}) \begin{pmatrix} z_3 \\ z_4 \\ f_1(z) \\ f_2(z) \end{pmatrix} \right)' \\ &\quad \cdot \text{diag}(I_2, M(z)^{-1}) \begin{bmatrix} 0 \\ 0 \\ 1 \\ 0 \end{bmatrix} \\ &= \left[0, 0, 1, \frac{s}{s+l} \right] \text{diag}(I_2, M(z)^{-1}) \begin{bmatrix} 0 \\ 0 \\ 1 \\ 0 \end{bmatrix} \\ &= \left[1, \frac{s}{s+l} \right] M(z)^{-1} \begin{bmatrix} 1 \\ 0 \end{bmatrix}. \end{aligned}$$

The latter expression is the high-frequency gain matrix

$$\Gamma : U_\beta \rightarrow \mathbf{GL}_1(\mathbb{R}),$$

$$\begin{aligned} x &\mapsto \left[1, \frac{s}{s+l} \right] M(x)^{-1} \begin{bmatrix} 1 \\ 0 \end{bmatrix} \\ &= \frac{36}{l^2 m (16 - 9 \cos^2(x_2))} \left[\frac{1}{3} - \frac{s}{l+s} \left(\frac{1}{3} + \frac{1}{2} \cos(x_2) \right) \right] \end{aligned}$$

which is invertible for $s = l$ since $x_2 \in \mathfrak{B}$ for all $x \in U_\beta$. Therefore, the relative degree of (5), (6) with $s = l$ is $r = 2$ on U_β . In passing, we mention the observation that for $s = l$ and $x \in \mathbb{R} \times [-\pi, \pi) \times \mathbb{R}^2$ we have $\Gamma(x) < 0$ if, and only if, $x \in U_\beta$, i.e., $x_2 \in \mathfrak{B}$. Since we seek to consider an open area around the equilibrium $x = 0$, where the relative degree is well defined, U_β is the largest set where this is true.

4. OUTPUT TRACKING CONTROL

In this section we present the novel controller design with which we perform the numerical case study in Section 5. First, as a motivation, we briefly recall the controller from Berger (2020) for linear non-minimum phase systems. Then, we derive the representation of system (5), (6) in Byrnes-Isidori form in order to isolate the internal dynamics. Based on the linearization of the internal dynamics we design a controller for end-effector output tracking of the manipulator.

4.1 Methodology

Recently, a controller for linear non-minimum phase systems was developed in Berger (2020). There, a differentially flat output y_{new} for the unstable part of the internal dynamics is introduced. Recall that all state and input variables can be parameterized in terms of a flat output, if

it exits, cf. Fliess et al. (1995). Interpreting the new output as output for a system with higher relative degree, the unstable part of the internal dynamics is removed. Then applying a funnel control law as in Berger et al. (2018) to the system with appropriate new reference signal leads to tracking with prescribed performance.

In order to adopt this approach for the robotic manipulator (5), (6) we first compute its internal dynamics based on the Byrnes-Isidori form (2). We then observe that the internal dynamics depend nonlinearly on \dot{y} and, when this is considered as the input, the unstable part does not have a flat output. Hence, we linearize the internal dynamics around the equilibrium and apply the above mentioned controller design based on this linearization. Since derivatives of the new output, which is defined in this way, are required we need to replace the variables obtained via the linearization with the variables of the original system. As an alternative, we present an approach where the derivatives are calculated using a high-gain observer.

4.2 Internal dynamics of the manipulator

Henceforth we consider end-effector tracking and set $s = l$. In order to obtain the internal dynamics, we transform system (5) with output (6) into Byrnes-Isidori form. For $U_\beta \subseteq \mathbb{R}^4$ as above, define $\Phi : U_\beta \rightarrow \mathbb{R}^4$ as in (3) with $\phi_i : U_\beta \rightarrow \mathbb{R}$, $i = 1, 2$. Since the distribution

$$\text{im } g(x) = \{0\}^2 \times \text{im } M(x)^{-1} \begin{bmatrix} 1 \\ 0 \end{bmatrix}$$

is one-dimensional and hence obviously involutive, we may choose ϕ_1 and ϕ_2 such that

$$\forall x \in U_\beta : 0 = (L_g \phi_i)(x) = \phi'_i(x) \text{diag}(I_2, M(x)^{-1}) \begin{bmatrix} 0 \\ 0 \\ 1 \\ 0 \end{bmatrix}. \quad (7)$$

Similar to the recent work Lanza (2021), we investigate the ansatz

$$\begin{aligned} \phi_1(x_1, \dots, x_4) &= \tilde{\phi}_1(x_1, x_2), \\ \text{and } \phi_2(x_1, \dots, x_4) &= \tilde{\phi}_2(x_1, x_2) \begin{pmatrix} x_3 \\ x_4 \end{pmatrix} \end{aligned}$$

for $\tilde{\phi}_1 : U_1 \rightarrow \mathbb{R}$, $\tilde{\phi}_2 : U_1 \rightarrow \mathbb{R}^{1 \times 2}$ and $U_1 = \mathbb{R} \times \mathfrak{B}$. Since we require the transformation Φ to be a local diffeomorphism, its Jacobian has to be invertible on U_β . This is the case if, and only if,

$$\begin{aligned} \forall x \in U_\beta : \Phi'(x) &= \begin{bmatrix} h'(x) \\ (h'f)'(x) \\ \phi'_1(x) \\ \phi'_2(x) \end{bmatrix} \\ &= \begin{bmatrix} [1, 1/2] & 0 \\ 0 & [1, 1/2] \\ \tilde{\phi}'_1(x_1, x_2) & 0 \\ * & \tilde{\phi}'_2(x_1, x_2) \end{bmatrix} \in \mathbf{GL}_4(\mathbb{R}) \\ \iff \forall q \in U_1 : & \begin{bmatrix} [1, 1/2] \\ \tilde{\phi}'_1(q) \end{bmatrix} \in \mathbf{GL}_2(\mathbb{R}) \\ & \wedge \begin{bmatrix} [1, 1/2] \\ \tilde{\phi}'_2(q) \end{bmatrix} \in \mathbf{GL}_2(\mathbb{R}). \end{aligned} \quad (8)$$

In order to satisfy conditions (7) and (8) we choose

$$\begin{aligned} \tilde{\phi}_1 : U_1 &\rightarrow \mathbb{R}, \quad q \mapsto q_2, \\ \tilde{\phi}_2 : U_1 &\rightarrow \mathbb{R}^{1 \times 2}, \quad q \mapsto \left[\frac{1}{3} + \frac{1}{2} \cos(q_2), \frac{1}{3} \right]. \end{aligned} \quad (9)$$

With this choice, clearly (7) is satisfied. In order to verify (8) we calculate

$$\begin{bmatrix} [1, 1/2] \\ \tilde{\phi}'_1(q) \end{bmatrix} = \begin{bmatrix} 1 & 1/2 \\ 0 & 1 \end{bmatrix} \quad \text{and} \quad \begin{bmatrix} [1, 1/2] \\ \tilde{\phi}'_2(q) \end{bmatrix} = \begin{bmatrix} 1 & \\ \frac{1}{3} + \frac{1}{2} \cos(q_2) & \frac{1}{3} \end{bmatrix}$$

for $q \in U_1$, where the latter is invertible since $q_2 \in \mathfrak{B}$. We may now infer that (5), (6) can be transformed into Byrnes-Isidori form with the particular choice for $\tilde{\phi}_1, \tilde{\phi}_2$ as in (9). Substituting the respective expressions via

$$\begin{pmatrix} y(t) \\ \dot{y}(t) \\ \eta_1(t) \\ \eta_2(t) \end{pmatrix} = \Phi \begin{pmatrix} \alpha(t) \\ \beta(t) \\ \dot{\alpha}(t) \\ \dot{\beta}(t) \end{pmatrix} \quad (10)$$

and rearranging yields

$$\begin{aligned} \begin{pmatrix} y(t) \\ \eta_1(t) \end{pmatrix} &= \begin{bmatrix} 1 & 1/2 \\ 0 & 1 \end{bmatrix} \begin{pmatrix} \alpha(t) \\ \beta(t) \end{pmatrix}, \\ \begin{pmatrix} \dot{y}(t) \\ \eta_2(t) \end{pmatrix} &= \begin{bmatrix} 1 & \\ \frac{1}{3} + \frac{1}{2} \cos(\beta(t)) & \frac{1}{3} \end{bmatrix} \begin{pmatrix} \dot{\alpha}(t) \\ \dot{\beta}(t) \end{pmatrix}. \end{aligned}$$

Solving the above equations for y, η_1 and \dot{y}, η_2 , we may now formulate the internal dynamics as in (2) as follows:

$$\begin{aligned} \dot{\eta}_1(t) &= g_{1,0}(\eta_1(t), \eta_2(t)) + g_{1,1}(\eta_1(t), \eta_2(t)) \dot{y}(t), \\ \dot{\eta}_2(t) &= g_{2,0}(\eta_1(t), \eta_2(t)) + g_{2,1}(\eta_1(t), \eta_2(t)) \dot{y}(t) \\ &\quad + g_{2,2}(\eta_1(t), \eta_2(t)) \dot{y}(t)^2, \end{aligned} \quad (11)$$

where $g_{i,j} : V \subseteq \mathbb{R}^2 \rightarrow \mathbb{R}$, $V = [0, I_2] \Phi(U_\beta)$ open, are appropriate functions with $g_{1,0}(0,0) = g_{2,0}(0,0) = 0$. The explicit representation can be found in Appendix A. Here we highlight that the internal dynamics depend nonlinearly on \dot{y} .

4.3 Controller design

The controller design is inspired by Berger (2020), and we apply these results to the internal dynamics. To this end, we linearize the internal dynamics (11) around the equilibrium $(\eta_1, \eta_2) = (0, 0)$, $\dot{y} = 0$ and obtain

$$\begin{pmatrix} \dot{\eta}_1(t) \\ \dot{\eta}_2(t) \end{pmatrix} = Q \begin{pmatrix} \eta_1(t) \\ \eta_2(t) \end{pmatrix} + P \dot{y}(t), \quad (12)$$

where

$$Q = \begin{bmatrix} 0 & -12 \\ -c & 12d \\ l^2 m & l^2 m \end{bmatrix}, \quad P = \begin{bmatrix} 10 \\ -10d \\ l^2 m \end{bmatrix}$$

and the matrix Q has eigenvalues

$$\begin{aligned} \lambda_1 &= \frac{6d}{l^2 m} - 2\sqrt{\left(\frac{3d}{l^2 m}\right)^2 + \frac{3c}{l^2 m}}, \\ \lambda_2 &= \frac{6d}{l^2 m} + 2\sqrt{\left(\frac{3d}{l^2 m}\right)^2 + \frac{3c}{l^2 m}}. \end{aligned}$$

Note, that for $c > 0$ we have $\lambda_1 < 0 < \lambda_2$, thus (12) has a hyperbolic equilibrium. Therefore, the linearized internal dynamics have an unstable part. Now, we find a transformation

$$V = \begin{bmatrix} \lambda_1 l^2 m & \lambda_2 l^2 m \\ \frac{c}{\lambda_1} & \frac{c}{\lambda_2} \end{bmatrix} \in \mathbf{GL}_2(\mathbb{R}),$$

which diagonalizes Q (and hence separates the stable and the unstable part of the internal dynamics) such that

$$V^{-1} Q V = \begin{bmatrix} \lambda_1 & 0 \\ 0 & \lambda_2 \end{bmatrix}, \quad V^{-1} P = \begin{bmatrix} p_1 \\ p_2 \end{bmatrix},$$

where $p_{1,2} = \pm \frac{10}{Dc}(c + d\lambda_{1,2})$, with $D := \frac{l^2 m}{c}(\lambda_1 - \lambda_2) = \det(V)$. Using the transformation $\hat{\eta}(t) = V^{-1}\eta(t)$ we obtain the linearized internal dynamics separated in a stable and an unstable part

$$\begin{aligned}\dot{\hat{\eta}}_1(t) &= \lambda_1 \hat{\eta}_1(t) + \frac{10}{Dc}(c + d\lambda_1)\dot{y}(t), \\ \dot{\hat{\eta}}_2(t) &= \lambda_2 \hat{\eta}_2(t) - \frac{10}{Dc}(c + d\lambda_2)\dot{y}(t).\end{aligned}\quad (13)$$

In virtue of Berger (2020) we seek to define an auxiliary output \hat{y}_{new} as a flat output for system (13), i.e., its second equation, and calculate the new relative degree of system (5) with respect to \hat{y}_{new} . However, it is not obvious how to treat this task. One way would be to express the new output in terms of the original coordinates (i.e., replace η_2 in (12) with η_2 in (11) and perform the same transformations which lead to $\hat{\eta}_2$) and calculate the derivatives. Another way, and this is the one we choose, is to use the linearization of the internal dynamics to calculate the relative degree based on (13). To avoid confusion we do not use the dot for time derivatives here, but a superscript to indicate the derivatives w.r.t. the linearization (13). The new output \hat{y}_{new} may be given by the variable of the unstable part as $\hat{y}_{\text{new}} = \hat{\eta}_2$, and we calculate

$$\begin{aligned}\hat{y}_{\text{new}}^{[1]}(t) &= \lambda_2 \hat{\eta}_2(t) + p_2 \dot{y}(t), \\ \hat{y}_{\text{new}}^{[2]}(t) &= \lambda_2 (\hat{\eta}_2(t) + p_2 \dot{y}(t)) + p_2 \ddot{y}(t).\end{aligned}$$

In the last equation we may insert the equation for \ddot{y} according to (5), (6), which explicitly depends on the input u . Hence, the relative degree of (5) with respect to \hat{y}_{new} is again $r_{\text{new}} = 2$, thus remains unchanged. Recalling the aim formulated in Section 4.1, we need to find a different output. To this end, we use the transformation $\bar{\eta}_2(t) = \hat{\eta}_2(t) - p_2 y(t)$ to obtain

$$\dot{\bar{\eta}}_2(t) = \lambda_2 \bar{\eta}_2(t) + \lambda_2 p_2 \dot{y}(t) \quad (14)$$

and define

$$y_{\text{new}}(t) = \bar{\eta}_2(t). \quad (15)$$

A short calculation shows that system (5) with new output (15) has relative degree $r_{\text{new}} = 3$:

$$\begin{aligned}y_{\text{new}}^{[1]}(t) &\stackrel{(14)}{=} \lambda_2 (\bar{\eta}_2(t) + p_2 y(t)) \\ y_{\text{new}}^{[2]}(t) &= \lambda_2^2 (\bar{\eta}_2(t) + p_2 y(t)) + \lambda_2 p_2 \dot{y}(t) \\ y_{\text{new}}^{[3]}(t) &= \lambda_2^3 (\bar{\eta}_2(t) + p_2 y(t)) + \lambda_2^2 p_2 \dot{y}(t) + \lambda_2 p_2 \ddot{y}(t),\end{aligned}\quad (16)$$

where in the last equation we again use (5), (6) to obtain the input u explicitly.

Remark 1. We stress that the derivatives $y_{\text{new}}^{[i]}$ are calculated by replacing the original unstable part of the internal dynamics, i.e., the second equation in (11), by the linearized version (14). They are not equivalent to those expressed in the original coordinates, which means that $y_{\text{new}}^{[1]}(t) \neq \dot{y}_{\text{new}}(t)$. More precisely, using the original coordinates would mean that the transformations leading from η_2 to $\bar{\eta}_2$ are performed with η_2 in (11) so that

$$\bar{\eta}_2 = \hat{\eta}_2 - p_2 y = [0, 1]V^{-1} \begin{pmatrix} \eta_1 \\ \eta_2 \end{pmatrix} - p_2 y, \quad (17)$$

and η_1, η_2, y are replaced via (10).

Now, in order to track the original reference with the original output, we have to find a new reference signal for system (5) with new output (15). The new reference \bar{y}_{ref}

is given by the solution of (14) when the original output y is substituted by the original reference signal y_{ref} :

$$\begin{aligned}\dot{\bar{\eta}}_{2,\text{ref}}(t) &= \lambda_2 \bar{\eta}_{2,\text{ref}}(t) + \lambda_2 p_2 y_{\text{ref}}(t), \quad \bar{\eta}_{2,\text{ref}}(0) = \bar{\eta}_{2,\text{ref}}^0 \\ \bar{y}_{\text{ref}}(t) &= \bar{\eta}_{2,\text{ref}}(t).\end{aligned}\quad (18)$$

We stress that (18) adds a dynamic equation to the overall controller design. In order for the controller from Berger et al. (2018) to be applicable, \bar{y}_{ref} and its derivatives should be bounded. To show this, we use the following well known result: there exists $x \in W^{1,\infty}(\mathbb{R}_{\geq 0} \rightarrow \mathbb{R})$ solving $\dot{x}(t) = \lambda x(t) + \gamma g(t)$, where $\lambda > 0, \gamma \in \mathbb{R}, g \in L^\infty(\mathbb{R}_{\geq 0} \rightarrow \mathbb{R})$, and $x(0) = x^0$ if, and only if, $x^0 + \int_0^\infty e^{-\lambda s} \gamma g(s) ds = 0$. Hence we set

$$\bar{\eta}_{2,\text{ref}}^0 = - \int_0^\infty e^{-\lambda_2 s} \lambda_2 p_2 y_{\text{ref}}(s) ds. \quad (19)$$

We emphasize that, if y_{ref} is generated by an exosystem

$$\dot{w}(t) = A_e w(t), \quad y_{\text{ref}}(t) = C_e w(t), \quad w(0) = w^0,$$

with known parameters $A_e \in \mathbb{R}^{k \times k}, C_e \in \mathbb{R}^{1 \times k}$ and $w^0 \in \mathbb{R}^k$ such that $\sigma(A_e) \subseteq \mathbb{C}_-$ and any eigenvalue $\lambda \in \sigma(A_e) \cap i\mathbb{R}$ is semisimple (note that this guarantees $y_{\text{ref}} \in W^{1,\infty}(\mathbb{R}_{\geq 0} \rightarrow \mathbb{R})$), then $\bar{\eta}_{2,\text{ref}}^0$ can be calculated via the solution $X \in \mathbb{R}^{1 \times k}$ of the Sylvester equation

$$Q_2 X - X A_e = P_2 C_e,$$

where in our example $Q_2 = \lambda_2$ and $P_2 = \lambda_2 p_2$. It is shown in (Berger, 2020, Lem. 3.2) that in this case

$$\bar{\eta}_{2,\text{ref}}^0 = -X w^0.$$

The tracking error for the auxiliary system with new output (15) and new reference (18) is defined by

$$e_0(t) = y_{\text{new}}(t) - \bar{y}_{\text{ref}}(t). \quad (20)$$

Applying the funnel control law from Berger et al. (2018) requires the derivatives of y_{new} , and in order to implement it we have to express them in terms of the original variables q . In the following we present two approaches to obtain these derivatives. In the first approach we use the representation in (16) and replace $\bar{\eta}_2$ by the original variables via (17) and (10). In the second approach we only replace y_{new} by the original variables and approximate the derivatives of this representation using a high-gain observer.

For later use and $\varphi_0 \in \Phi_3, \kappa_0 > 0$, we define the expressions

$$\begin{aligned}e_0^{[1]} &= y_{\text{new}}^{[1]} - \dot{\bar{y}}_{\text{ref}}, \\ e_0^{[2]} &= y_{\text{new}}^{[2]} - \ddot{\bar{y}}_{\text{ref}}, \\ k_0^{[1]} &= \frac{2\kappa_0 \varphi_0 e_0}{(1 - \varphi_0^2 e_0^2)^2} \left(\dot{\varphi}_0 e_0 + \varphi_0 e_0^{[1]} \right), \\ e_1^{[1]} &= e_0^{[2]} + k_0 e_0^{[1]} + k_0^{[1]} e_0.\end{aligned}\quad (21)$$

Linearization. The first option is to replace $\bar{\eta}_2$ in y_{new} and its derivatives in (16) by (17) and to express everything in terms of the original coordinates via (10). To this end, we consider

$$\begin{aligned}\Psi : U_\beta &\rightarrow \mathbb{R} \\ (x_1, \dots, x_4) &\mapsto -p_2(x_1 + \frac{1}{2}x_2) \\ &\quad + \frac{1}{D} \left(-x_2 + \frac{\lambda_2 l^2 m}{c} \left[\left(\frac{1}{3} + \frac{1}{2} \cos(x_2) \right) x_3 + \frac{1}{3} x_4 \right] \right)\end{aligned}$$

and replace $\bar{\eta}_2(t) = \Psi(\alpha(t), \beta(t), \dot{\alpha}(t), \dot{\beta}(t))$ in $y_{\text{new}}(t) = \bar{\eta}_2(t)$ and in (16), thus

$$\begin{aligned}
y_{\text{new}}(t) &= \Psi(\alpha(t), \beta(t), \dot{\alpha}(t), \dot{\beta}(t)), \\
y_{\text{new}}^{[1]}(t) &= \lambda_2 \Psi(\alpha(t), \beta(t), \dot{\alpha}(t), \dot{\beta}(t)) + \lambda_2 p_2(\alpha(t) + \frac{1}{2}\beta(t)), \\
y_{\text{new}}^{[2]}(t) &= \lambda_2^2 \Psi(\alpha(t), \beta(t), \dot{\alpha}(t), \dot{\beta}(t)) + \lambda_2^2 p_2(\alpha(t) + \frac{1}{2}\beta(t)) \\
&\quad + \lambda_2 p_2(\dot{\alpha}(t) + \frac{1}{2}\dot{\beta}(t)). \tag{22}
\end{aligned}$$

With this, the application of the controller from Berger et al. (2018) to system (5) with new output (15) and reference signal as in (18) leads to the following overall control law:

$$\begin{aligned}
\dot{\bar{\eta}}_{2,\text{ref}}(t) &= \lambda_2 \bar{\eta}_{2,\text{ref}}(t) + \lambda_2 p_2 y_{\text{ref}}(t), \quad \bar{\eta}_{2,\text{ref}}(0) = \bar{\eta}_{2,\text{ref}}^0, \\
\bar{y}_{\text{ref}}(t) &= \bar{\eta}_{2,\text{ref}}(t), \\
y_{\text{new}}(t) &= \Psi(\alpha(t), \beta(t), \dot{\alpha}(t), \dot{\beta}(t)), \\
e_0(t) &= y_{\text{new}}(t) - \bar{y}_{\text{ref}}(t), \\
e_1(t) &= e_0^{[1]}(t) + k_0(t)e_0(t), \quad e_0^{[1]} \text{ via (21) and (22)}, \\
e_2(t) &= e_1^{[1]}(t) + k_1(t)e_1(t), \quad e_1^{[1]} \text{ via (21) and (22)}, \\
k_i(t) &= \frac{1}{1 - \varphi_i(t)^2 e_i(t)^2}, \quad i = 0, 1, 2, \\
u(t) &= k_2(t)e_2(t), \tag{23}
\end{aligned}$$

with $\bar{\eta}_{2,\text{ref}}^0$ as in (19), reference signal $y_{\text{ref}} \in W^{1,\infty}(\mathbb{R}_{\geq 0} \rightarrow \mathbb{R})$ and funnel functions $\varphi_i \in \Phi_{3-i}$ for $i = 0, 1, 2$. Note that, since $\Gamma(x)$ is negative for $x \in U_\beta$, the control input u has a positive sign according to Berger et al. (2018).

High-gain observer. The second option is to approximate the first and second derivative of y_{new} using a high-gain observer, see Khalil (2001). To this end, consider

$$\dot{\zeta}(t) = L(y_{\text{new}}(t) - \zeta_1(t)) + Z\zeta(t), \quad \zeta(0) = \zeta^0 \in \mathbb{R}^3,$$

where

$$Z = \begin{bmatrix} 0 & I_2 \\ 0 & 0 \end{bmatrix}, \quad L = \begin{bmatrix} l_1 \\ l_2 \\ l_3 \end{bmatrix},$$

with $l_i \in \mathbb{R}$ for $i = 1, 2, 3$. Then ζ_2 and ζ_3 approximate the first and second derivative of y_{new} , thus for the controller we set $y_{\text{new}}^{[1]} = \zeta_2$ and $y_{\text{new}}^{[2]} = \zeta_3$. The high-gain observer is a dynamical part of the controller and invoking (21) the overall controller reads:

$$\begin{aligned}
\dot{\bar{\eta}}_{2,\text{ref}}(t) &= \lambda_2 \bar{\eta}_{2,\text{ref}}(t) + \lambda_2 p_2 y_{\text{ref}}(t), \quad \bar{\eta}_{2,\text{ref}}(0) = \bar{\eta}_{2,\text{ref}}^0, \\
\bar{y}_{\text{ref}}(t) &= \bar{\eta}_{2,\text{ref}}(t), \\
y_{\text{new}}(t) &= \Psi(\alpha(t), \beta(t), \dot{\alpha}(t), \dot{\beta}(t)), \\
\dot{\zeta}_1(t) &= l_1(y_{\text{new}}(t) - \zeta_1(t)) + \zeta_2(t), \quad \zeta_1(0) = \zeta_1^0 \\
\dot{\zeta}_2(t) &= l_2(y_{\text{new}}(t) - \zeta_1(t)) + \zeta_3(t), \quad \zeta_2(0) = \zeta_2^0 \\
\dot{\zeta}_3(t) &= l_3(y_{\text{new}}(t) - \zeta_1(t)), \quad \zeta_3(0) = \zeta_3^0 \\
y_{\text{new}}^{[1]}(t) &= \zeta_2(t), \\
y_{\text{new}}^{[2]}(t) &= \zeta_3(t), \\
e_0(t) &= y_{\text{new}}(t) - \bar{y}_{\text{ref}}(t) \\
e_1(t) &= e_0^{[1]}(t) + k_0(t)e_0(t), \quad e_0^{[1]} \text{ via (21)}, \\
e_2(t) &= e_1^{[1]}(t) + k_1(t)e_1(t), \quad e_1^{[1]} \text{ via (21)}, \\
k_i(t) &= \frac{1}{1 - \varphi_i(t)^2 e_i(t)^2}, \quad i = 0, 1, 2, \\
u(t) &= k_2(t)e_2(t), \tag{24}
\end{aligned}$$

with $\bar{\eta}_{2,\text{ref}}^0$ as in (19), high-gain observer parameters $l_i \in \mathbb{R}$ and initial values $\zeta_i^0 \in \mathbb{R}$, $i = 1, 2, 3$, reference signal $y_{\text{ref}} \in W^{1,\infty}(\mathbb{R}_{\geq 0} \rightarrow \mathbb{R})$ and funnel functions $\varphi_i \in \Phi_{3-i}$ for $i = 0, 1, 2$.

5. NUMERICAL CASE STUDY

In this section we present the results of the numerical case study. We perform end-effector output tracking of the manipulator arm (5) with $l = 1$ m, $m = 1$ kg, $c = 1$ Nm/rad and $d = 0.25$ Nms/rad applying controls (23) and (24), resp. As a reference signal we choose the trajectory from Seifried and Blajer (2013)

$$\begin{aligned}
y_{\text{ref}}(t) &= y_0 + \left[126\left(\frac{t}{t_f-t_0}\right)^5 - 420\left(\frac{t}{t_f-t_0}\right)^6 + 540\left(\frac{t}{t_f-t_0}\right)^7 \right. \\
&\quad \left. - 315\left(\frac{t}{t_f-t_0}\right)^8 + 70\left(\frac{t}{t_f-t_0}\right)^9 \right] (y_f - y_0),
\end{aligned}$$

which establishes a transition from y_0 to y_f within the time interval t_0 to t_f . The situation is depicted in Figure 3.

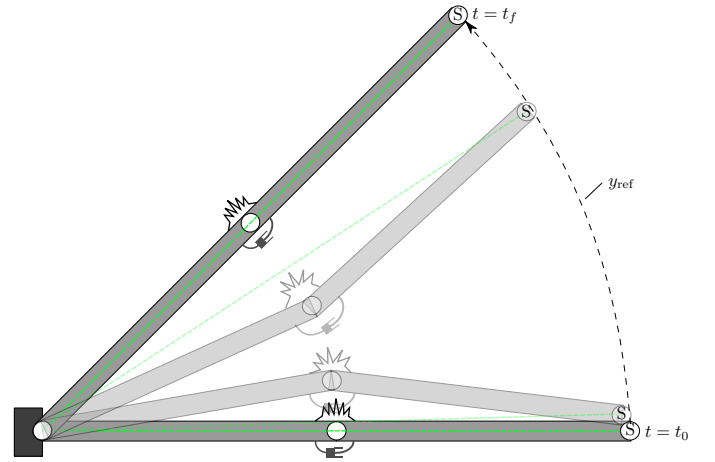


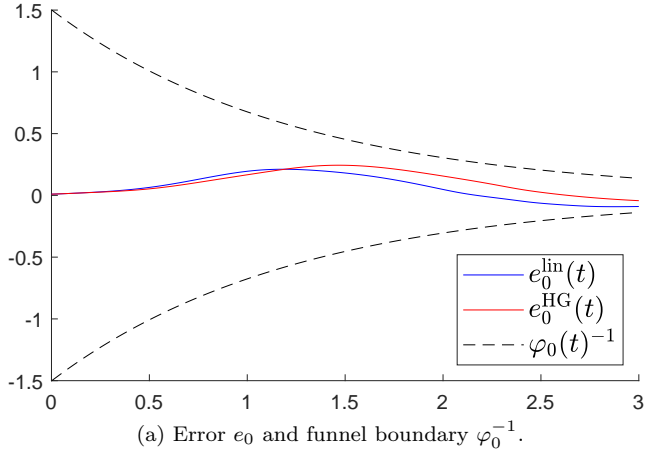
Fig. 3: Schematic snapshots of the manipulator arm's transition established by the reference trajectory y_{ref} with $y_0 = 0$ rad and $y_f = \frac{\pi}{4}$ rad.

We choose $y_0 = 0$ rad, $y_f = \frac{\pi}{4}$ rad, $t_0 = 0$ s and $t_f = 3$ s, which means the transition is performed in rather short time, namely within three seconds. We choose the funnel functions

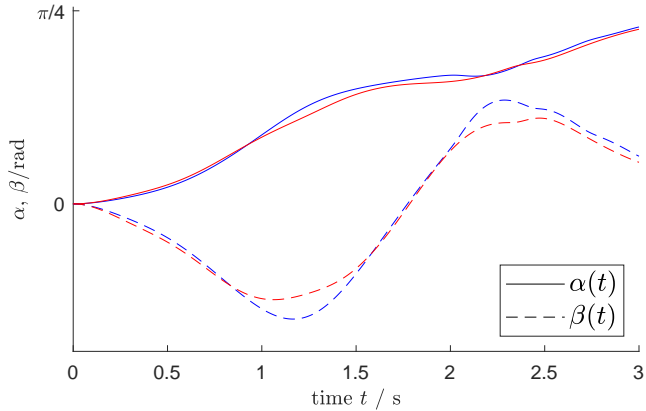
$$\begin{aligned}
\varphi_0(t) &= \varphi_1(t) = (1.5e^{-0.8t} + 0.001)^{-1}, \\
\varphi_2(t) &= (60e^{-0.2t} + 0.001)^{-1}, \quad t \geq 0,
\end{aligned}$$

which ensure that the initial errors $e_0(0), e_1(0), e_2(0)$ lie within the respective funnel boundaries; and we choose the high-gain parameters $l_1 = 10^2, l_2 = 10^5, l_3 = 10^6$. Furthermore, we assume the control torque to be affected by high frequent disturbances $d(t)$ as expectable in real applications caused e.g. by friction or unexpected external vibrating forces, cf. (Hackl, 2017, Ch. 11 & 13). For simulation purposes we choose $d(t) = 0.1 \sin(5t) + 0.2 \cos(8t)$ and recall that in (5) we have $u_d(t) = u(t) + d(t)$.

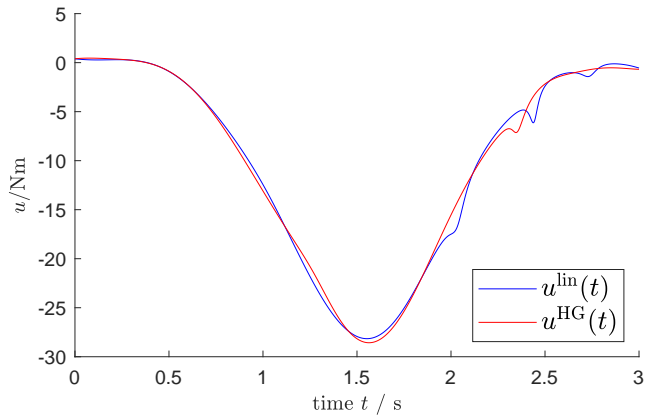
Figure 4 shows the results of the simulations, which have been performed in MATLAB (solver: ode15s, rel. tol.: 10^{-9} , abs. tol.: 10^{-12}) over the time interval $0 - 3$ s. In the following the superscript *lin* refers to the results under the control (23), where the derivatives of y_{new} are expressed via (22); the superscript *HG* refers to the results under



(a) Error e_0 and funnel boundary φ_0^{-1} .



(b) Angles α and β of the manipulator arm.



(c) Input function u .

Fig. 4. Simulation of the controllers (23) (superscript *lin*) and (24) (superscript *HG*) applied to (5), (6) under disturbances d .

the control (24), where the derivatives of y_{new} are approximated via a high-gain observer. As depicted in Figure 4a the error e_0 evolves within the funnel boundary φ_0^{-1} . Figure 4b shows the state variables, i.e., the angles (α , β), of system (5) during the tracking process. The large angle β , i.e., large deflection of the passive link, results from the fast transition within three seconds. However, note that $\beta(t) \in \mathfrak{B}$ for $0 \leq t \leq 3$. In Figure 4c the respective control inputs u are depicted. Note that both approaches, the linearization and the use of a high-gain observer, generate comparable control inputs. Figure 5 shows that the goal

of the numerical case study, namely end-effector output tracking of a prescribed trajectory, is successful.

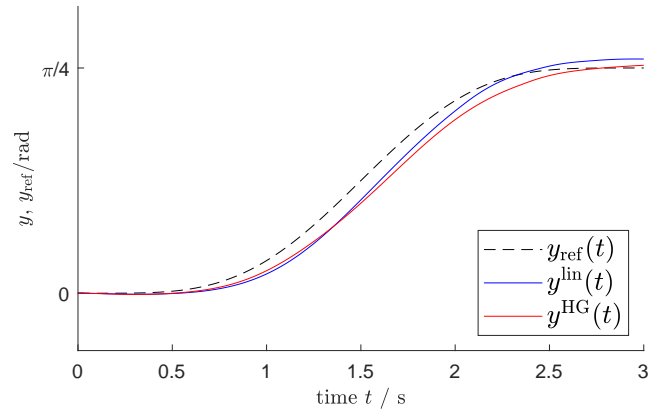


Fig. 5: Output y and reference y_{ref} .

6. CONCLUSION

In the present paper we exploited ideas and methods recently found for linear non-minimum phase systems in Berger (2020) to proceed a numerical case study for a nonlinear non-minimum phase robotic manipulator. To this end, we transformed the system under consideration into Byrnes-Isidori form in order to decouple the internal dynamics. We linearized the internal dynamics around an equilibrium point and separated its stable and unstable parts. Then we followed the steps in the aforementioned work in order to design the feedback control laws (23) and (24) using different methods to approximate the new output's derivatives. Utilizing these control laws we simulated end-effector output tracking of the rotational manipulator arm (5). The simulation showed that output tracking of such a nonlinear non-minimum phase system is successful, even under the action of disturbances.

We stress that the present paper is only a case study in order to gain some insight as to whether the methods and ideas derived in Berger (2020) can be extended to nonlinear non-minimum phase systems. The presented results give reason to adopt the presented techniques to achieve efficient control methods for nonlinear systems with unstable internal dynamics via funnel control.

REFERENCES

- Berger, T. (2020). Tracking with prescribed performance for linear non-minimum phase systems. *Automatica*, 115, Article 108909.
- Berger, T., Breiten, T., Puche, M., and Reis, T. (2021a). Funnel control for the monodomain equations with the FitzHugh-Nagumo model. *J. Diff. Eqns.*, 286, 164–214.
- Berger, T., Ilchmann, A., and Ryan, E.P. (2021b). Funnel control of nonlinear systems. *Math. Control Signals Syst.*, 33, 151–194.
- Berger, T., Lê, H.H., and Reis, T. (2018). Funnel control for nonlinear systems with known strict relative degree. *Automatica*, 87, 345–357.
- Berger, T., Otto, S., Reis, T., and Seifried, R. (2019). Combined open-loop and funnel control for underactuated multibody systems. *Nonlinear Dynamics*, 95, 1977–1998.

- Berger, T. and Rauert, A.L. (2018). A universal model-free and safe adaptive cruise control mechanism. In *Proceedings of the MTNS 2018*, 925–932. Hong Kong.
- Berger, T. and Rauert, A.L. (2020). Funnel cruise control. *Automatica*, 119, Article 109061.
- Berger, T. and Reis, T. (2014). Zero dynamics and funnel control for linear electrical circuits. *J. Franklin Inst.*, 351(11), 5099–5132.
- Chen, D. and Paden, B. (1996). Stable inversion of nonlinear non-minimum phase systems. *Int. J. Control*, 64(1), 81–97.
- Devasia, S., Chen, D., and Paden, B. (1996). Nonlinear inversion-based output tracking. *IEEE Trans. Autom. Control*, 41(7), 930–942.
- Fliess, M., Levine, J., Martin, P., and Rouchon, P. (1995). Flatness and defect of non-linear-systems: introductory theory and examples. *Int. J. Control*, 61, 1327–1361.
- Gopalswamy, S. and Hedrick, J.K. (1993). Tracking nonlinear non-minimum phase systems using sliding control. *Int. J. Control*, 57(5), 1141–1158.
- Hackl, C.M. (2014). Funnel control for wind turbine systems. In *Proc. 2014 IEEE Int. Conf. Contr. Appl., Antibes, France*, 1377–1382.
- Hackl, C.M. (2015). Current PI-funnel control with anti-windup for synchronous machines. In *Proc. 54th IEEE Conf. Decis. Control, Osaka, Japan, 1997–2004*.
- Hackl, C.M. (2017). *Non-identifier Based Adaptive Control in Mechatronics—Theory and Application*. Springer-Verlag, Cham, Switzerland.
- Hackl, C.M., Endisch, C., and Schröder, D. (2008). Funnel-Control in robotics: An introduction. In *Proc. 16th Mediterranean Conf. Control & Automation, Ajaccio, France*, 913–919.
- Hackl, C.M. and Kennel, R.M. (2012). Position funnel control for rigid revolute joint robotic manipulators with known inertia matrix. In *20th Mediterranean Conf. Control & Automation, Barcelona, Spain*, 615–620.
- Ilchmann, A., Ryan, E.P., and Sangwin, C.J. (2002). Tracking with prescribed transient behaviour. *ESAIM: Control, Optimisation and Calculus of Variations*, 7, 471–493.
- Ilchmann, A. and Trenn, S. (2004). Input constrained funnel control with applications to chemical reactor models. *Syst. Control Lett.*, 53(5), 361–375.
- Ilchmann, A. and Wirth, F. (2013). On minimum phase. *Automatisierungstechnik*, 12, 805–817.
- Isidori, A. (1995). *Nonlinear Control Systems*. Communications and Control Engineering Series. Springer-Verlag, Berlin, 3rd edition.
- Isidori, A. (2000). A tool for semiglobal stabilization of uncertain non-minimum-phase nonlinear systems via output feedback. *IEEE Trans. Autom. Control*, 45(10), 1817–1827.
- Khalil, H.K. (2001). *Nonlinear Systems*. Prentice-Hall, Upper Saddle River, NJ, 3rd edition.
- Lanza, L. (2021). Internal dynamics of multibody systems. *Syst. Control Lett.* To appear. Preprint available from arXiv: <https://arxiv.org/abs/2009.08726v2>.
- Marconi, L., Isidori, A., and Serrani, A. (2004). Non-resonance conditions for uniform observability in the problem of nonlinear output regulation. *Syst. Control Lett.*, 53(3–4), 281–298.
- Nazrulla, S. and Khalil, H. (2009). Output regulation of non-minimum phase nonlinear systems using an extended high-gain observer. In *Proc. 2009 IEEE Int. Conf. Control Automation*, 732–737.
- Pomprapa, A., Weyer, S., Leonhardt, S., Walter, M., and Misgeld, B. (2015). Periodic funnel-based control for peak inspiratory pressure. In *Proc. 54th IEEE Conf. Decis. Control, Osaka, Japan*, 5617–5622.
- Seifried, R. and Blajer, W. (2013). Analysis of servo-constraint problems for underactuated multibody systems. *Mech. Sci.*, 4, 113–129.
- Shkolnikov, I.A. and Shtessel, Y.B. (2002). Tracking in a class of nonminimum-phase systems with nonlinear internal dynamics via sliding mode control using method of system center. *Automatica*, 38(5), 837–842.

Appendix A. THE FUNCTIONS $g_{i,j}$

Here we list the functions $g_{i,j}$ that appear in (11).

$$g_{1,0} : V \subseteq \mathbb{R}^2 \rightarrow \mathbb{R},$$

$$(\eta_1, \eta_2) \mapsto \frac{12}{2 - 3 \cos(\eta_1)} \eta_2,$$

$$g_{1,1} : V \subseteq \mathbb{R}^2 \rightarrow \mathbb{R},$$

$$(\eta_1, \eta_2) \mapsto \frac{-12}{2 - 3 \cos(\eta_1)} \left(\frac{1}{3} + \frac{1}{2} \cos(\eta_1) \right),$$

$$g_{2,0} : V \subseteq \mathbb{R}^2 \rightarrow \mathbb{R},$$

$$(\eta_1, \eta_2) \mapsto \frac{-1}{l^2 m (2 - \cos(\eta_1))^2} \cdot \left\{ \eta_1 [4c - 12c + 9c \cos(\eta_1)^2] + 4\eta_2 [6d - 9(d \cos(\eta_1) + l^2 m \eta_2 \sin(\eta_1))] \right\},$$

$$g_{2,1} : V \subseteq \mathbb{R}^2 \rightarrow \mathbb{R},$$

$$(\eta_1, \eta_2) \mapsto \frac{2}{l^2 m (2 - \cos(\eta_1))^2 (16 - 9 \cos(\eta_1)^2)} \cdot \left\{ \eta_2 [453 \sin(\eta_1) + 216 \sin(2\eta_1) - 27 \sin(3\eta_1) + l^2 m \left(\frac{-1071}{2} \sin(\eta_1) - \frac{1071}{4} \sin(2\eta_1) + \frac{81}{4} \sin(3\eta_1) + \frac{81}{8} \sin(4\eta_1) \right)] + \frac{35d}{8} - \frac{99d}{2} \cos(2\eta_1) + \frac{81d}{8} \cos(4\eta_1) \right\},$$

$$g_{2,2} : V \subseteq \mathbb{R}^2 \rightarrow \mathbb{R},$$

$$(\eta_1, \eta_2) \mapsto \frac{-4 \sin(\eta_1)}{l^2 m (2 - \cos(\eta_1))^2 (16 - 9 \cos(\eta_1)^2)} \cdot \left\{ 80 + 144 \cos(\eta_1) + 90 \cos(\eta_1)^2 - [80 + 192 \cos(\eta_1) + 90 \cos(\eta_1)^2 - 27 \cos(\eta_1)^3] l^2 m \right\}.$$